



Cite this: *Analyst*, 2020, **145**, 5166

Interactions between gold, thiol and As(III) for colorimetric sensing†

Junling Duan,^{a,b} Biwu Liu^b and Juewen Liu  ^{*b}

As(III) or arsenite is extremely toxic, and various colorimetric sensors were reported for its on-site detection. A highly cited example was based on gold nanoparticles (AuNPs) modified with a few thiol-containing compounds including dithiothreitol (DTT), reduced glutathione (GSH), and cysteine (Cys). As(III) was believed to crosslink these surface ligands to aggregate AuNPs and produce a red-to-blue color change. Since As(III) can also adsorb on AuNPs, we herein carefully studied this effect on these ligand-capped AuNPs. For citrate-capped AuNPs, 10 mM free citrate resulted in a strong blue color in the presence of As(III) attributable to the elevated ionic strength, while common divalent cations resulted in no color change due to the chelation effect of free citrate. For AuNPs capped with the three thiol compounds, more than 5 mM As(III) was needed to produce a color change, which was very different from the previously reported color change with nanomolar concentration of As(III). Our color change was attributed to the displacement of the surface ligands by As(III) instead of crosslinking by it. This conclusion was made based on the irreversibility of the color change, kinetics of the reaction, and high As(III) concentration needed. This work has revealed that any two species from AuNPs, thiol and As(III) can react. It also calls for care in the interpretation of related colorimetric sensing mechanisms, and the need to consider the previously overlooked As(III) adsorption onto AuNPs.

Received 10th May 2020,
Accepted 29th June 2020

DOI: 10.1039/d0an00946f
rsc.li/analyst

Introduction

Arsenic is a contaminant in water posing serious health concerns to exposed people.^{1,2} The most important inorganic arsenic species include As(III) and As(V), which have quite different properties. As(V) is chemically similar to phosphate, while As(III) is a softer ligand with affinity to many soft metals and proteins. As(III) tends to adsorb onto noble metals such as gold and silver,³ while As(V) has a high affinity to various metal oxides such as iron oxide.⁴ Overall, As(III) is more toxic and many methods have been developed for its detection,⁵ including Raman spectroscopy,⁶ inductively-coupled plasma mass spectrometry,⁷ atomic absorption spectrometry,⁸ fluorometric spectrometry,^{4,9,10} electrochemistry,^{11–13} and colorimetric methods.^{14,15}

Using gold nanoparticles (AuNPs) to develop colorimetric sensors by taking advantage of their very high extinction coefficients and distance-dependent color^{16–25} has been extensively reported.^{26–28} Many AuNP-based arsenic sensors used thiol-containing molecules to functionalize AuNPs²⁹ and used As(III) to induce aggregation of AuNPs, producing a color change.^{26,27}

We have recently shown that As(III) can also adsorb onto AuNPs.³ In addition, As(III) can strongly interact with thiol, which is one of the chemical reasons for its toxicity.¹ As(III) binding by three cysteine residues in proteins was reported.³⁰ In another example, As(III) was used to bind to a peptide containing three cysteine residues, which prevented the adsorption of the peptide onto AuNPs.²⁸ Therefore, AuNPs, thiol and As(III) form an interesting system, where each two can bind.

However, adsorption of As(III) onto AuNPs has not been considered in previous sensing work. We have recently shown that such an interaction adversely affected an aptamer and AuNP based sensing system.^{3,31} Herein, we studied a few ligands commonly used to cap AuNPs, including citrate and various thiol-containing small molecules such as glutathione (GSH), dithiothreitol (DTT), and cysteine (Cys). We paid particular attention to the adsorption of As(III) onto AuNPs. Our results do not support As(III) crosslinking AuNPs capped with these

^aCollege of Chemistry and Material Science, Shandong Agricultural University, Tai'an, Shandong 271018, P.R. China

^bDepartment of Chemistry, Waterloo Institute for Nanotechnology, University of Waterloo, Waterloo, Ontario N2L 3G1, Canada. E-mail: liujw@uwaterloo.ca; Fax: +1 (519)-746-0435; Tel: +1 (519) 888-4567

† Electronic supplementary information (ESI) available. See DOI: [10.1039/d0an00946f](https://doi.org/10.1039/d0an00946f)

ligands, although adsorbed As(III) can influence the colloidal stability of AuNPs and a high concentration of As(III) can displace these ligands.

Materials and methods

Chemicals

HAuCl₄, HAsNa₂O₄·7H₂O, AsNaO₂, dithiothreitol (DTT), reduced L-glutathione (GSH), cysteine (Cys), and 5,5'-dithiobis(2-nitrobenzoic acid, DTNB, Ellman's reagent) were purchased from Sigma Aldrich. Citric acid and trisodium citrate were purchased from Mandel Scientific (Guelph, ON, Canada). AuNPs (50 nm) were purchased from Ted Pella Inc. Milli-Q water was used for preparing all the solutions.

Synthesis and modification of 13 nm AuNPs

Citrate-capped AuNPs (13 nm) were synthesized according to the previously reported method,³² and the particle concentration of the as-prepared AuNPs was ~10 nM. The AuNPs were modified with GSH, DTT, and Cys according to the previous report with some modifications.²⁶ In brief, 40 µL of GSH (10 mM), DTT (10 mM) and Cys (0.1 mM) were separately added to 6 mL of AuNPs (1.5 nM) with stirring for 2 h. Then, the modified AuNPs were kept for 12 h without disturbance. Subsequently, the modified AuNPs were centrifuged and redispersed in 1.5 mL of Milli-Q water for further use. At this point, the particle concentration of the modified AuNPs was ~6 nM.

Colorimetric assays using AuNPs

Different concentrations of metal ions were added to 50 µL of citrate-capped AuNPs (~6 nM) or thiol-capped AuNPs (~6 nM), and the particle concentration of the final AuNPs was ~3.7 nM. After incubation for 0.5 h, the UV-vis spectra were obtained using a spectrophotometer (Agilent 8458A) and the color was also recorded using a digital camera.

Reaction of thiol compounds with DTNB

Stock solutions of DTT and GSH were prepared freshly just before use. The DTNB stock solution (2 mM) was prepared with a final concentration of 50 mM sodium acetate. The concentrations of DTT and GSH were detected by adding 50 µL of DTNB solution (2 mM) and 100 µL of Tris buffer (1 M, pH 7.5). The final volume was adjusted to 1 mL. The absorbance at 412 nm (A_{412}) was measured after 5 min of incubation at room temperature. The A_{412} value was proportional to the DTT/GSH concentration.

Reaction of As(III) with thiols

First, different concentrations of As(III) were respectively mixed with DTT (40 µM) or GSH (80 µM). After carrying out the reaction for a certain time, the DTT/GSH solution with As(III) was mixed with 50 µL of DTNB solution (2 mM) and 100 µL of Tris buffer (1 M, pH 7.5). The A_{412} value was measured after 5 min of incubation.

Results and discussion

Citrate-capped AuNPs: opposite color changes by As(III) and metal ions

We first diluted the as-synthesized 13 nm citrate-capped AuNPs in water to reach an absorbance of ~1.0 at 520 nm, which corresponds to a concentration of ~3.7 nM AuNPs. The dispersed AuNPs were red in color. We then respectively added As(III) and a few divalent metal ions to the AuNPs. A slight color change occurred with 1 mM As(III), while obvious aggregation and purple/blue color were observed with 1 mM Pb²⁺, Cd²⁺, Cu²⁺, or Ca²⁺ (Fig. 1A). It needs to be pointed out that As(III) exists as an anion (arsenite, AsO₃³⁻) in water, which is very different from the tested metal cations.

The as-synthesized AuNPs contained a low concentration of citrate (~3 mM), which was diluted to ~0.9 mM since we diluted the AuNPs by 3.3-fold for this experiment. Since citrate may act as a metal chelator and mask the added metal ions, we further tested the effect of citrate. We added an additional 10 mM citrate (pH 6.6, containing 30 mM Na⁺ since trisodium citrate was used). In this case, only the color of the As(III) added sample changed to blue at a relatively low concentration (10 µM As(III)), whereas all the cation added samples remained red even at 1 mM (Fig. 1B). Therefore, the added citrate likely masked the cations by chelation.

To quantitatively understand the effect of As(III), we titrated As(III) to the 10 mM citrate added AuNPs and monitored the reaction using UV-vis spectrometry (Fig. 1D, black squares). The freshly prepared AuNPs in the dispersed state had a strong surface plasmon peak at 520 nm, whereas the aggregated AuNPs had stronger extinction at around 620 nm. Therefore, this figure plotted the extinction ratio at these two wavelengths with a high ratio indicative of aggregated AuNPs of blue color. The color change started with just 5 µM As(III), while 10 µM As(III) saturated the color change, which is consistent with the color change observed in the photograph. For comparison, the as-synthesized AuNPs showed no color change when the As(III) concentration was below 100 µM (Fig. 1D, blue triangles), and their color changed only when the As(III) concentration was higher than 5 mM (Fig. 1E, black trace). Therefore, the extra 10 mM citrate destabilized the AuNPs against As(III) by over 1000-fold. Yet at the same time, the added citrate stabilized the AuNPs against the metal cations. When larger AuNPs of 50 nm were used (Fig. 1E, blue trace), we also observed that more than 40 mM As(III) was needed to induce aggregation. Since the 13 nm AuNPs are most often used, the rest of this study was focused on them.

The stability constants ($\log K$) of metal(M)/citrate complexes for the equation $M^{2+} + cit^{3-} = Mcit^-$ were 7.35 (Cu²⁺), 5.47 (Pb²⁺), 4.87 (Cd²⁺) and 4.77 (Ca²⁺).^{33,34} Therefore, with 10 mM citrate, 1 mM of these metal ions can be effectively masked. As(III) being an anion was not affected by citrate, but Na⁺ in the added citrate buffer increased the ionic strength. We reason that As(III) displaced the surface citrate to destabilize AuNPs in a high ionic strength solution. While this observation might be useful for the colorimetric detection of As(III), we did not

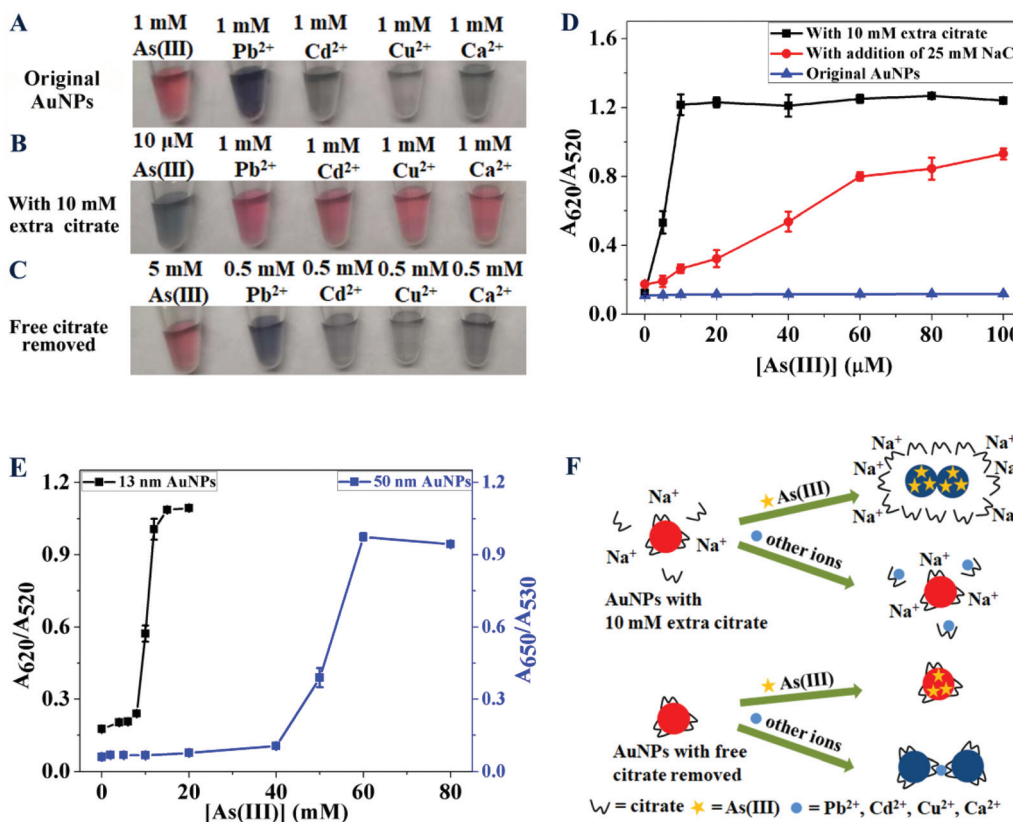


Fig. 1 Photographs of AuNPs with various metal ions and As(III) added: (A) with the citrate-capped AuNPs; (B) with the citrate-capped AuNPs in the presence of additional 10 mM citrate; (C) with the washed AuNPs and free citrate removed. (D) The light extinction ratio of the three types of AuNPs with different concentrations of As(III) added. (E) The extinction ratio of the citrate-capped AuNPs after adding different concentrations of As(III). (F) Cartoon representation of the effect of As(III) and metal cations to the AuNPs with no citrate or 10 mM citrate. As(III) can displace the surface citrate, and AuNPs would aggregate if the ionic strength is high.

pursue detection further in this work. Other species that can destabilize AuNPs based on this mechanism can also cause a similar color change, such as Br^- , I^- , dopamine, and adenosine.^{35,36} To test our hypothesis, we added an additional 25 mM NaCl to the as-synthesized AuNPs (adding more NaCl would aggregate AuNPs), and then titrated As(III). We added NaCl to separate the effects of Na^+ and the citrate anion. In this sample, we also observed the aggregation of the AuNPs with only 10 μM As(III) (Fig. 1D, red dots). This experiment supported that the extra Na^+ provided by sodium citrate was the main reason for the increased sensitivity to As(III).

Since the added extra citrate decreased the tolerance of AuNPs to As(III), we then tried to decrease the citrate concentration. We washed the as-prepared AuNPs by centrifugation and dispersed them in water to fully remove citrate. Interestingly, all the metal cations caused aggregation at 0.5 mM. Some metal ions, such as Pb^{2+} ,³⁷ can bridge the surface citrate to aggregate the AuNPs (although bulk citrate was removed, a layer of adsorbed citrate could still exist).^{38,39} For metal ions with a lower affinity to citrate, they can serve as a general electrolyte to increase the ionic strength and screen the negative charges on the AuNPs, also inducing aggregation. Interestingly, the citrate-removed sample remained red even

with 5 mM As(III) (Fig. 1C). This can be explained by the lack of a high ionic strength to induce aggregation. Therefore, the concentration of free citrate clearly determined the effect of the added metal cations. We summarized these results schematically in Fig. 1F.

GSH, Cys and DTT-capped AuNPs

After understanding the citrate-capped AuNPs, we then prepared GSH-capped AuNPs. GSH could displace citrate since it has a thiol group.⁴⁰ Free GSH and citrate were washed away by centrifugation, and then As(III) or other metal ions were added. In this case, the samples turned blue at lower metal concentrations such as 50 μM Pb^{2+} , Cd^{2+} , or Cu^{2+} , or 500 μM Ca^{2+} , while the color remained red when a much higher concentration of As(III) was added (Fig. 2A). In fact, the AuNPs remained red even with 10 mM As(III) (Fig. 2A, the first tube). The color changed to blue only when the As(III) concentration reached 60 mM, and the apparent K_d of this reaction was around 50 mM As(III) (Fig. 2B).

Similarly, we respectively prepared DTT- and Cys-capped AuNPs, and exposed them to the ions. As shown in Fig. 2C and Fig. 2D, 10 mM As(III) did not cause the aggregation of these AuNPs. All the other metal ions caused the aggregation of

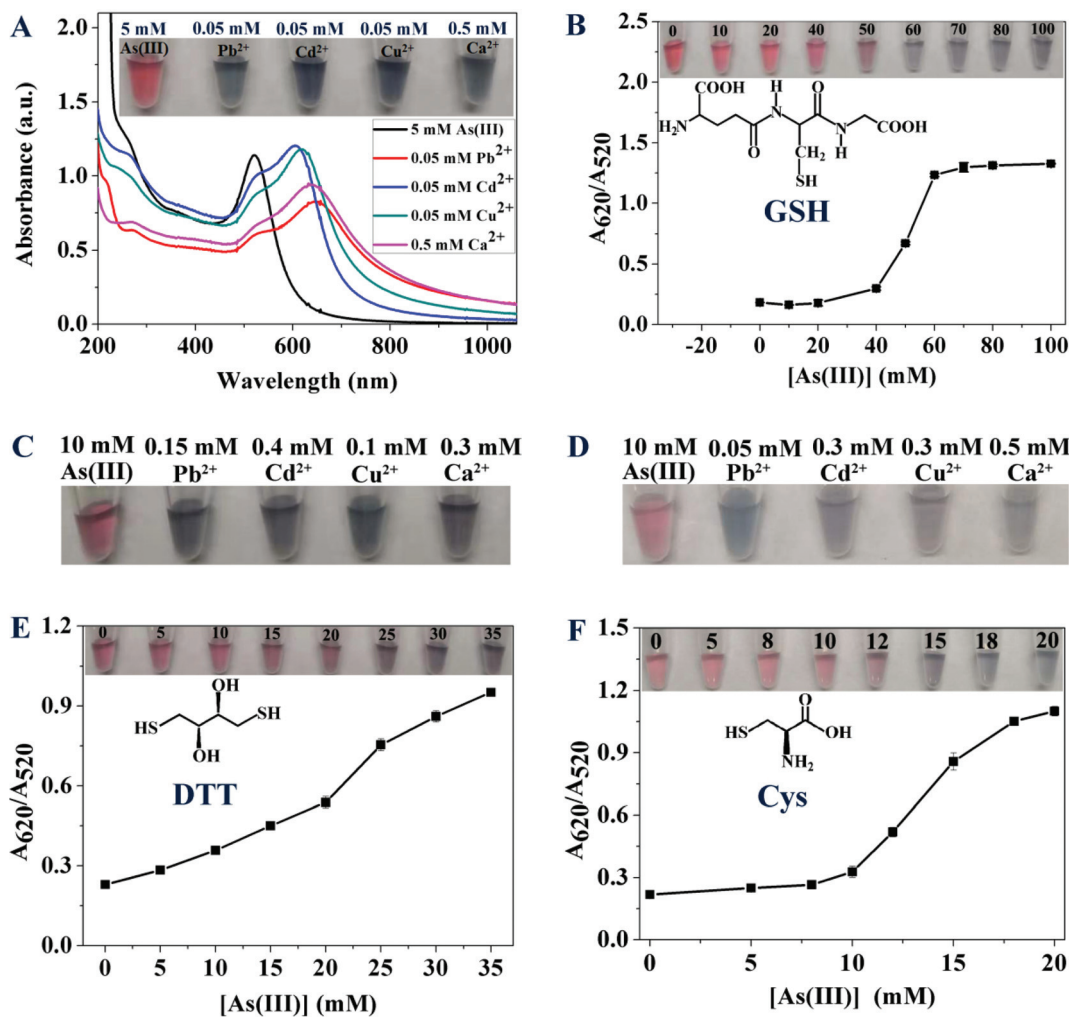


Fig. 2 (A) UV-vis spectra of the GSH-capped AuNPs in the presence of different metal ions and the corresponding photographs (inset). (B) The extinction ratio of the GSH-AuNPs with different concentrations of As(III). (C) Photographs of DTT-capped AuNPs and (D) cysteine-capped AuNPs containing various metal ions. The absorbance ratio of (E) DTT-capped AuNPs and (F) Cys-capped AuNPs. The insets of B, E, and F are the corresponding photographs with As(III) concentration marked in mM, and the structures of GSH, DTT and Cys.

AuNPs at below 0.5 mM, although some metal ions were more sensitive to certain ligands. For example, 50 μ M Pb²⁺ caused the aggregation of the Cys-capped AuNPs, while 150 μ M Pb²⁺ was needed for the DTT-capped AuNPs. Nevertheless, the overall trends were similar to that of the GSH-capped AuNPs.

We further titrated As(III) to the DTT-capped AuNPs (Fig. 2E) and the Cys-capped AuNPs (Fig. 2F). The extinction ratio increased with increasing As(III) concentrations. 25 mM As(III) aggregated the DTT-capped AuNPs, while 15 mM As(III) aggregated the Cys-capped AuNPs. Therefore, for the AuNPs capped with these thiol containing molecules, more than 10 mM As(III) was required to aggregate, whereas less than 0.5 mM of the cations was sufficient. Interestingly, this trend was opposite to that of the citrate-capped AuNPs.

As(III) bridged or As(III) displacement mechanism

Although our results were consistent with those reported in the literature in terms of As(III)-induced aggregation of GSH,

DTT and Cys-capped AuNPs, the As(III) concentration was very different. In the paper by Kalluri *et al.*,²⁶ the apparent K_d for the aggregation of AuNPs functionalized with a mixture of GSH, DTT and Cys was about 400 parts-per-trillion (5.3 nM) As(III). Although dynamic light scattering (DLS) was used for their quantification, the measurement was still based on the aggregation of the AuNPs and the K_d value should be useful for comparison. In our current work, all the three ligands had apparent K_d values above 5 mM, with a discrepancy of more than 6 orders of magnitude. Kalluri *et al.* explained their observation by the carboxylate groups in GSH and Cys for binding to As(III) as schematically shown in Fig. 3A. Yet, they cited stability constants referring to the thiol/As(III) interactions. It is unlikely that the carboxyl or hydroxyl groups can strongly bind As(III) (e.g. stronger than thiol binding). DTT has two thiols and Kalluri *et al.* proposed that one of the thiols was anchored on AuNPs, while the other interacted with As(III). We reason it is more likely that both thiol ligands

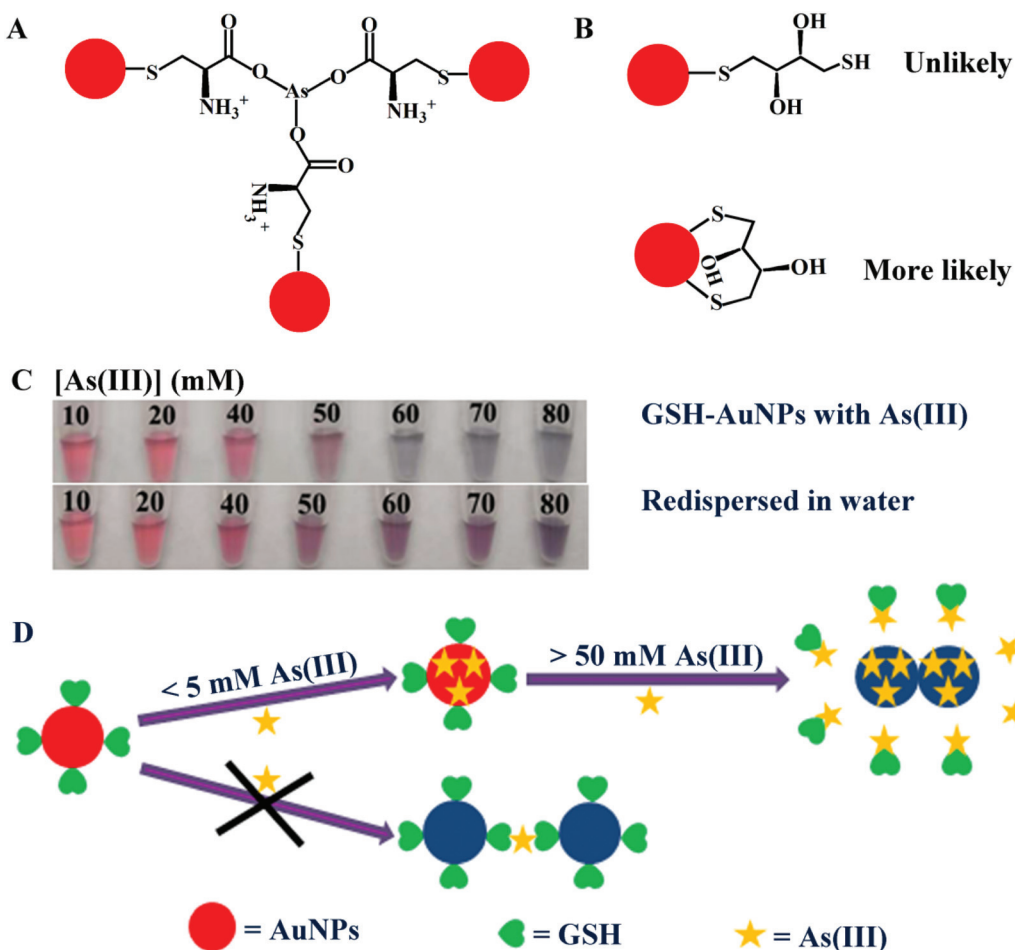


Fig. 3 (A) Scheme of As(III) binding to Cys-capped AuNPs. Redrawn based on ref. 26. (B) Possible ways of DTT adsorption on AuNPs. (C) Photograph of the GSH-capped AuNPs with different concentrations of As(III) and then redispersed in water. (D) Graphical representation of As(III) displacing GSH from AuNPs, while no evidence supported As(III)-mediated aggregation.

would interact with AuNPs to achieve a chelation effect (Fig. 3B).⁴¹

When thiol/As(III) binding is considered, the affinity varied quite a lot in the literature using different measurement methods. DTT could bind As(III) at around pH 6–7 in aqueous solutions.^{42–44} Most papers reported a low micromolar K_d value (e.g. 0.3–1 μ M for As(III)/DTT).^{45,46} Thus, the K_d value for As(III) binding to carboxylate groups should be even higher. Therefore, low nM As(III) is unlikely to react with these ligand-capped AuNPs. Our results requiring more than 5 mM As(III) for DTT may not be explained by the simple thiol/As(III) binding either.

At such a high As(III) concentration, its displacement of the adsorbed GSH from AuNPs might occur. It is possible that As(III) competed with GSH (or Cys and DTT) for the AuNP surface, which induced aggregation. Such aggregation should be irreversible. To test this, we washed the As(III) aggregated GSH-AuNPs and re-dispersed it in water. All the samples initially with more than 50 mM As(III) were still aggregated after washing as shown by the purple color (Fig. 3C), indicating that the aggregation was irreversible. Although the

samples with 60–80 mM As(III) changed color from blue to purple after re-dispersion in water, this was attributed to the large aggregates broken into smaller ones due to the lowering of the ionic strength. For reversible aggregation, the color should revert back to red. If As(III)'s effect were to crosslink GSH, one would expect reversible aggregation. When the As(III) concentration dropped, the AuNPs would disassemble immediately. However, we observed irreversible aggregation. Therefore, the As(III)-induced aggregation was the result of another mechanism and we believe it was due to the displacement of the surface ligand as shown in Fig. 3D. With this mechanism, we can explain the need for high mM As(III). Only with such excess As(III), can it compete with the thiol group on the AuNPs.

Colorimetric assay of As(III)/thiol interactions

The above studies indicated strong interactions between As(III) and AuNPs to displace the adsorbed thiol. Another driving force for this reaction could be from As(III)/thiol interactions. The reaction between thiol and As(III) has been extensively studied,⁴³ for example by NMR under a nitrogen atmosphere

forming $\text{As}(\text{III})(\text{SG})_3$.⁴⁷ Isothermal titration calorimetry (ITC) was previously used but it required high concentrations of both thiol and $\text{As}(\text{III})$. In our experiment, the thiol concentration was quite low (overall below 1 μM attached to the 3.7 nM AuNPs), and those measurements cannot be used. So, we needed a new method to reflect our experimental conditions.

We used the Ellman's reagent (DTNB) to develop a simple colorimetric method. DTNB is colorless, but after reacting with free thiol, it produces a yellow color (Fig. 4A). Therefore, it can quantify the free thiol concentration. We first calibrated the free thiol in DTT (Fig. S1†) and GSH (Fig. S2†). For both com-

pounds, the absorbance of the DTNB complex increased linearly with increasing thiol concentration. Since DTT has two thiols, twice concentration of GSH resulted in a similar absorbance to that of DTT.

When DTT and GSH were treated with $\text{As}(\text{III})$ before adding DTNB, the absorbance of DTNB decreased owing to the loss of free thiol attributable to $\text{As}(\text{III})$ /thiol binding (Fig. 4C). A low absorbance of the DTT/DTNB complex was observed when DTT was first treated with 40 μM $\text{As}(\text{III})$ for 1 h. While for the GSH/DTNB system, higher concentrations of $\text{As}(\text{III})$ (e.g. 80 mM) were needed to react with GSH (Fig. 4D and E). Fig. 4B

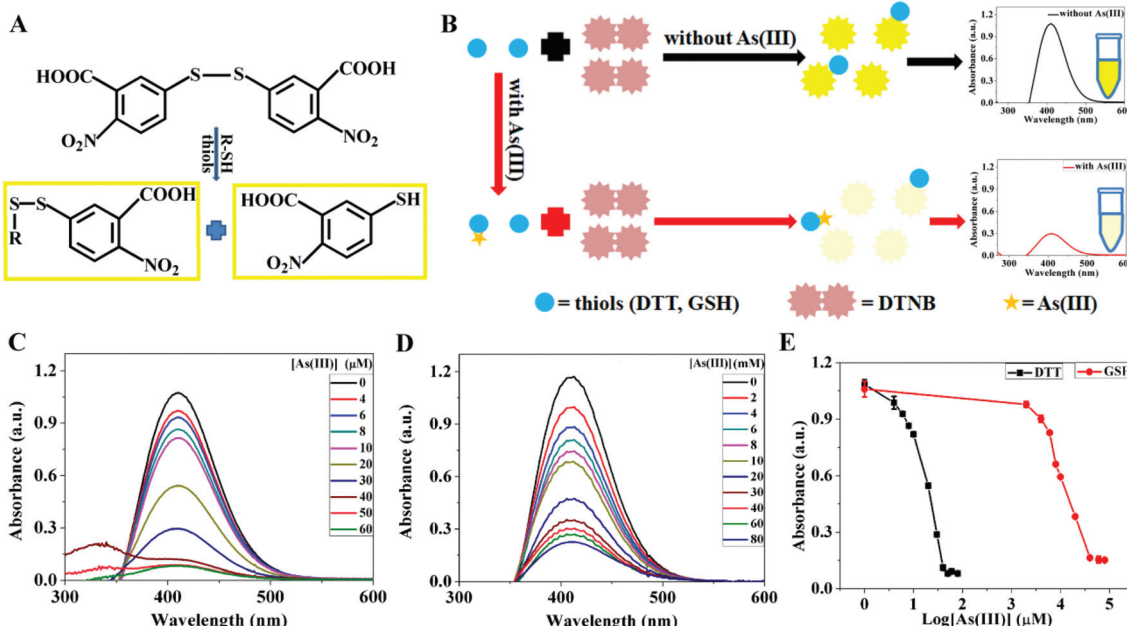


Fig. 4 (A) The reaction between free thiol and DTNB producing yellow products. (B) A scheme of reactions between thiols and DTNB without and with $\text{As}(\text{III})$. (C) The UV-vis spectra of DTT-DTNB mixture in the presence of different concentrations of $\text{As}(\text{III})$ (reaction time: 1 h). (D) The UV-vis spectra of GSH-DTNB mixture in the presence of different concentrations of $\text{As}(\text{III})$ (reaction time: 3 h). (E) The absorbance of the DTT-DTNB and GSH-DTNB mixtures at different concentrations of $\text{As}(\text{III})$.

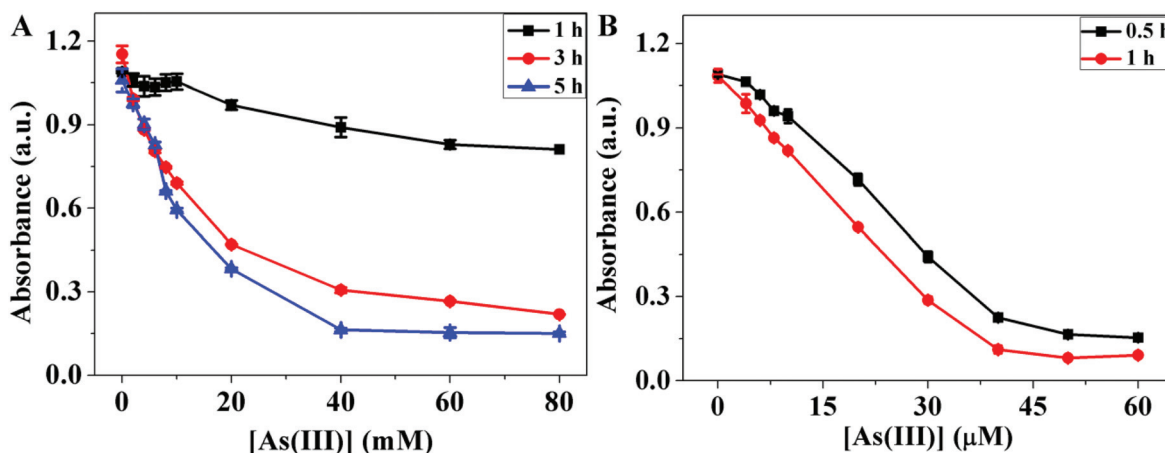


Fig. 5 The absorbance of the (A) GSH-DTNB, and (B) DTT-DTNB mixtures in the presence of different concentrations of $\text{As}(\text{III})$ at different reaction times.

illustrates the interaction of DTT/GSH with DTNB in the presence of As(III).

A key reason for DTT having tighter binding is due to the chelation effect, and this is consistent with the literature.^{42,46} Therefore, DTNB can provide a simple colorimetric assay for studying thiol/As(III) binding. Here, DTT reacted with As(III) at three orders of magnitude lower concentration (Fig. 4E), but in the above AuNP assays, the required As(III) concentration for DTT-capped AuNPs was still in the mM range. Therefore, a high concentration of As(III) was needed to displace DTT.

Kinetics of the thiol/As(III) reaction

We then studied the kinetics of the reaction between thiol and As(III) by pre-incubating As(III) and thiol for various times before adding DTNB. As shown in Fig. 5A, only a little change in the absorbance was observed when GSH and As(III) were reacted for 1 h. However, during 3–5 h of reaction before adding DTNB, high concentrations of As(III) resulted in significant reaction with GSH. Therefore, the reaction between GSH and DTNB was slow and needed a long time when compared with the reaction between As(III) and DTT which was much faster. After reaction with As(III) for 1 h, the absorbance of DTT-DTNB complex decreased a lot (Fig. 5B). Since the red-to-blue color change of the GSH-capped AuNPs induced by a high concentration of As(III) occurred within 1 min, much shorter than the binding reaction in Fig. 5A, this kinetic evidence also pointed to the displacement of the GSH ligand by As(III).

Conclusions

In summary, we have carefully studied various ligand-capped AuNPs in the presence of As(III), and a few divalent metal cations were used for comparison. We have made the following observations. First, As(III) cannot crosslink GSH, DTT or Cys-capped AuNPs. The aggregation of AuNPs was observed only with more than 10–50 mM As(III). DTT had a 1000-fold stronger affinity than GSH for As(III), but still a similarly high As(III) concentration was required to aggregate the AuNPs capped with these ligands. This indicated that the reaction was dominated by the As(III)/AuNP interaction instead of As(III)/thiol binding. Our observations do not support the previous As(III) colorimetric sensing mechanism, nor could we repeat the reported color change sensitive to a very low concentration of As(III) in the nanomolar region.²⁶ Second, the As(III)/AuNP interaction appeared very important. The aggregation was attributed to the competition between As(III) and thiol for the gold surface. Adsorption of As(III) onto the silver surfaces has been more studied in SERS-based As(III) detection,^{6,48–50} but the interaction between As(III) and gold was less explored.³ We observed that a low concentration of As(III) can displace citrate, while a high concentration of As(III) can even displace thiol. Finally, for the citrate-capped AuNPs, the effect of free citrate needs to be taken into consideration. They can mask many divalent metal ions. We only observed that arsenic can selectively aggregate the citrate-capped AuNPs in the presence of extra 10 mM

citrate or extra NaCl. The sodium in citrate or NaCl increased the ionic strength. The added As(III) can displace the surface citrate and aggregate the AuNPs with increased ionic strength. Therefore, the effects of free ligands, surface ligands and target/AuNP interactions are all critical and they need to be taken into consideration for developing colorimetric sensors.

Conflicts of interest

There are no conflicts to declare.

Acknowledgements

We thank the financial support from the Natural Sciences and Engineering Research Council of Canada (NSERC) and the National Natural Science Foundation of China (No. 21607096). J. Duan was supported by the Chinese Scholarship Council (CSC) as a visiting scholar to the University of Waterloo.

References

- 1 S. Shen, X. F. Li, W. R. Cullen, M. Weinfeld and X. C. Le, *Chem. Rev.*, 2013, **113**, 7769–7792.
- 2 D. K. Nordstrom, *Science*, 2002, **296**, 2143–2145.
- 3 C. Zong, Z. Zhang, B. Liu and J. Liu, *Langmuir*, 2019, **35**, 7304–7311.
- 4 B. Liu and J. Liu, *Chem. Commun.*, 2014, **50**, 8568–8570.
- 5 L. Zhang, X. R. Chen, S. H. Wen, R. P. Liang and J. D. Qiu, *TrAC, Trends Anal. Chem.*, 2019, **118**, 869–879.
- 6 M. Mulvihill, A. Tao, K. Benjauthrit, J. Arnold and P. Yang, *Angew. Chem., Int. Ed.*, 2008, **47**, 6456–6460.
- 7 V. Dufailly, L. Noël and T. Guérin, *Anal. Chim. Acta*, 2008, **611**, 134–142.
- 8 F. L. Pantuzzo, J. C. J. Silva and V. S. T. Ciminelli, *J. Hazard. Mater.*, 2009, **168**, 1636–1638.
- 9 K. Ge, J. Liu, P. Wang, G. Fang, D. Zhang and S. Wang, *Microchim. Acta*, 2019, **186**, 197.
- 10 L. Zhang, X. Z. Cheng, L. Kuang, A.-Z. Xu, R. P. Liang and J. D. Qiu, *Biosens. Bioelectron.*, 2017, **94**, 701–706.
- 11 T. Gupte, S. K. Jana, J. S. Mohanty, P. Srikrishnarka, S. Mukherjee, T. Ahuja, C. Sudhakar, T. Thomas and T. Pradeep, *ACS Appl. Mater. Interfaces*, 2019, **11**, 28154–28163.
- 12 D. Kato, T. Kamata, D. Kato, H. Yanagisawa and O. Niwa, *Anal. Chem.*, 2016, **88**, 2944–2951.
- 13 L. Yang, B. An, X. Yin and F. Li, *Chem. Commun.*, 2020, **56**, 5311–5314.
- 14 S.-H. Wen, R.-P. Liang, L. Zhang and J.-D. Qiu, *ACS Sustainable Chem. Eng.*, 2018, **6**, 6223–6232.
- 15 S. H. Wen, X. L. Zhong, Y. D. Wu, R. P. Liang, L. Zhang and J. D. Qiu, *Anal. Chem.*, 2019, **91**, 6487–6497.
- 16 K. Saha, S. S. Agasti, C. Kim, X. Li and V. M. Rotello, *Chem. Rev.*, 2012, **112**, 2739–2779.

17 A. B. Chinen, C. M. Guan, J. R. Ferrer, S. N. Barnaby, T. J. Merkel and C. A. Mirkin, *Chem. Rev.*, 2015, **115**, 10530–10574.

18 W. Zhao, M. A. Brook and Y. Li, *ChemBioChem*, 2008, **9**, 2363–2371.

19 J. Liu, Z. Cao and Y. Lu, *Chem. Rev.*, 2009, **109**, 1948–1998.

20 B. Liu and J. Liu, *Matter*, 2019, **1**, 825–847.

21 K. Shrivastav, R. Shankar and K. Dewangan, *Sens. Actuators, B*, 2015, **220**, 1376–1383.

22 R. Dominguez-Gonzalez, L. Gonzalez Varela and P. Bermejo-Barrera, *Talanta*, 2014, **118**, 262–269.

23 N. Priyadarshni, P. Nath, Nagahanumaiah and N. Chanda, *ACS Sustainable Chem. Eng.*, 2018, **6**, 6264–6272.

24 T. Yang, X.-X. Zhang, J.-Y. Yang, Y.-T. Wang and M.-L. Chen, *Talanta*, 2018, **177**, 212–216.

25 B. S. Boruah, R. Biswas and P. Deb, *Opt. Laser Technol.*, 2019, **111**, 825–829.

26 J. R. Kalluri, T. Arbneshi, S. Afrin Khan, A. Neely, P. Candice, B. Varisli, M. Washington, S. McAfee, B. Robinson, S. Banerjee, A. K. Singh, D. Senapati and P. C. Ray, *Angew. Chem., Int. Ed.*, 2009, **48**, 9668–9671.

27 J. Li, L. Chen, T. Lou and Y. Wang, *ACS Appl. Mater. Interfaces*, 2011, **3**, 3936–3941.

28 N. Xia, Y. Shi, R. Zhang, F. Zhao, F. Liu and L. Liu, *Anal. Methods*, 2012, **4**, 3937–3941.

29 J. C. Love, L. A. Estroff, J. K. Kriebel, R. G. Nuzzo and G. M. Whitesides, *Chem. Rev.*, 2005, **105**, 1103–1169.

30 D. S. Touw, C. E. Nordman, J. A. Stuckey and V. L. Pecoraro, *Proc. Natl. Acad. Sci. U. S. A.*, 2007, **104**, 11969–11974.

31 C. Zong and J. Liu, *Anal. Chem.*, 2019, **91**, 10887–10893.

32 J. Liu and Y. Lu, *Nat. Protoc.*, 2006, **1**, 246–252.

33 S. J. Markich and P. L. Brown, *Thermochemical Data for Environmentally-Relevant Elements*, Australia, 1999, p. 138.

34 R. E. Farrell, J. J. Germida and P. M. Huang, *Appl. Environ. Microbiol.*, 1990, **56**, 3006–3016.

35 B. Liu, P. Wu, Z. Huang, L. Ma and J. Liu, *J. Am. Chem. Soc.*, 2018, **140**, 4499–4502.

36 X. Liu, F. He, F. Zhang, Z. Zhang, Z. Huang and J. Liu, *Anal. Chem.*, 2020, **92**, 9370–9378.

37 G. Zhong, J. Liu and X. Liu, *Micromachines*, 2015, **6**, 462–472.

38 J.-W. Park and J. S. Shumaker-Parry, *J. Am. Chem. Soc.*, 2014, **136**, 1907–1921.

39 J.-W. Park and J. S. Shumaker-Parry, *ACS Nano*, 2015, **9**, 1665–1682.

40 R. Wu, L.-P. Jiang, J.-J. Zhu and J. Liu, *Langmuir*, 2019, **35**, 13461–13468.

41 T. B. Creczynski-Pasa, M. A. D. Millone, M. L. Munford, V. R. de Lima, T. O. Vieira, G. A. Benitez, A. A. Pasa, R. C. Salvarezza and M. E. Vela, *Phys. Chem. Chem. Phys.*, 2009, **11**, 1077–1084.

42 A. Kolozsi, A. Lakatos, G. Galbács, A. Ø. Madsen, E. Larsen and B. Gyuresik, *Inorg. Chem.*, 2008, **47**, 3832–3840.

43 N. A. Rey, O. W. Howarth and E. C. Pereira-Maia, *J. Inorg. Biochem.*, 2004, **98**, 1151–1159.

44 M. Delnomdedieu, M. M. Basti, J. D. Ottos and D. J. Thomas, *Chem.-Biol. Interact.*, 1994, **90**, 139–155.

45 A. M. Spuches, H. G. Kruszyna, A. M. Rich and D. E. Wilcox, *Inorg. Chem.*, 2005, **44**, 2964–2972.

46 W. L. Zahler and W. W. Cleland, *J. Biol. Chem.*, 1968, **243**, 716–719.

47 N. Scott, K. M. Hatlelid, N. E. MacKenzie and D. E. Carter, *Chem. Res. Toxicol.*, 1993, **6**, 102–106.

48 M. W. Yang, Q. L. Zou, D. J. Chen, J. Hu, Q. H. Lin and H. M. Zhu, *Langmuir*, 2020, **36**, 1662–1670.

49 M. W. Yang, V. Liamtsau, C. J. Fang, K. L. Sylvers, A. J. McGoron, G. L. Liu, F. F. Fu and Y. Cai, *Anal. Chem.*, 2019, **91**, 8280–8288.

50 S. Y. Xu, W. Q. Tang, D. B. Chase, D. L. Sparks and J. F. Rabolt, *ACS Appl. Nano Mater.*, 2018, **1**, 1257–1264.